Molecular Vision 2025; 31:440-452 <http://www.molvis.org/molvis/v31/440>
Received 9 October 2024 | Accepted 8 November 2025 | Published 10 November 2025

© 2025 Molecular Vision

System biology analysis reveals that Grm6 is associated with glutamate accumulation–induced scotopic vision impairment in diabetic mice

Ying Lian,[1,2] Yanpu Zhao,[3,4] Xiaoyu Yang,[3,4] Hongjie He,[3,4] Zhanyi Yang,[3,4] Huanhuan Zhang,[3,4] Guigang Yan,[2] Lu Lu,[5] Jia Mi,[3,4] Geng Tian,[3,4] Yanping Zhu[3,4]

(The first three authors contributed equally to this work.)

[1]The Second Clinical School, Binzhou Medical University, Yantai, Shandong, China; [2]Department of Ophthalmology, Yantai Yuhuangding Hospital Affiliated to Qingdao University, Yantai, Shandong, China; [3]School of Pharmacy, Binzhou Medical University, Yantai, Shandong, China; [4]Shandong Technology Innovation Center of Molecular Targeting and Intelligent Diagnosis and Treatment, Yantai, Shandong, China; [5]Department of Genetics, Genomics and Informatics, The University of Tennessee Health Science Center, Memphis, TN

Purpose: Scotopic vision impairment as an early event is found in diabetic retinopathy. However, the underlying mechanisms behind hyperglycemia-induced scotopic vision impairment remain unclear. This study aims to identify that Grm6 is associated with glutamate accumulation–induced scotopic vision impairment under hyperglycemia.
Methods: In this study, diabetic mice with impaired scotopic vision were induced by streptozotocin, and the retinal electrical activity was evaluated using electroretinography. Label-free quantitative proteomic analysis was used to identify differentially expressed proteins in the retinas of diabetic mice. A retinal transcriptome-wide association analysis and correlation screening were performed in BXD mice strains to explore the potential genes associated with hyperglycemia. Gene function enrichment analysis was used to evaluate gene function and to construct the correlation network.
Results: In total, 151 proteins were significantly altered in the retina of diabetic mice. Among these 151 candidates, 22 genes presented a significant correlation with blood glucose level ($p<0.05$), which were enriched in alanine, aspartate, and glutamate metabolism ($p=0.003$). Moreover, the glutamate catabolism-related genes Slc1a2, Gad1, and Glud1 were significantly negatively correlated with blood glucose at the transcript and proteome levels, which led to glutamate accumulation under hyperglycemia. Among eight types of metabotropic glutamate receptors, Grm6 had the most significant correlation with blood glucose level ($R=-0.5291$, $p=0.0003$). Moreover, Grm6 expression was significantly decreased at both the mRNA and protein levels in the diabetic retina. Gene coexpression network analysis further identified that Grm6 was correlated with Rgs9, suggesting that hyperglycemia may impair scotopic vision via the phototransduction pathway.
Conclusions: Our study confirms that Grm6 is associated with scotopic vision impairment induced by glutamate accumulation in diabetic mice and provides an efficient strategy for exploring critical biomarkers and pathways through a combination of proteomics and transcriptome-wide association analysis.

As one of the most common complications of diabetes, diabetic retinopathy (DR) is associated with irreversible visual impairments and blindness [1,2]. Approximately 30% of diabetic patients develop DR, and among these patients, about 10% progress to proliferative diabetic retinopathy or diabetic macular edema. These complications are the most vision-threatening and can lead to irreversible blindness if left untreated [3,4]. DR was initially considered a pure microvascular disease, with microvascular structural changes and fluid extravasation. However, this hypothesis cannot provide a sufficient explanation for symptoms such as scotopic vision loss in the early DR, suggesting alternative mechanisms are involved.

The development of advanced imaging techniques, particularly optical coherence tomography angiography, has highlighted retinal neurodegeneration as an early event in DR, driven by chronic hyperglycemia [5,6]. In DR, retinal neurodegeneration is often accompanied by scotopic vision impairment, and such visual deficits typically precede the onset of microvascular abnormalities [7]. Clinical evidence also demonstrates that compared with normal blood glucose controls, elevated glucose levels in patients with prediabetes and type 2 diabetes are associated with significant reductions in scotopic electroretinography (ERG) amplitudes [8]. Scotopic vision impairment in DR may originate from dysregulation of the rod phototransduction cascade, particularly involving regulator of G-protein signaling 9 (RGS9).

Correspondence to: Yanping Zhu, Binzhou Medical University, Guanhai Road 346, Laishan District, 264003, Yantai, Shandong, China, email: yanpingzhu1983@163.com

As a GTPase-activating protein of the RGS family, RGS9 catalyzes the hydrolysis of GTP in G protein–phosphodiesterase complexes to terminate phototransduction signals in rod photoreceptors, which are essential for scotopic vision [9]. However, the exact molecular pathway linking hyperglycemic stress to RGS9-mediated impairments in phototransduction termination remains incompletely elucidated, highlighting the need for further mechanistic investigations.

Recently, the transcriptome-wide association (TWAS) approach has emerged to investigate the molecular mechanisms of chronic diseases [10]. It collects transcriptomic and phenotypic data from either human populations or genetic reference populations (GRPs) of animal models. Through appropriate bioinformatics analyses, the constructed transcriptome–phenotype correlation network will help identify novel biomarkers and pathways to reveal disease mechanisms. Among currently available GRPs, the BXD recombinant inbred mouse panel stands as a well established, efficient, and exceptionally data-rich genetic reference population, derived from the systematic inbreeding of offspring from a cross between the parental strains C57BL/6J (B6) and DBA/2J (D2). Currently, the BXD recombinant inbred strains comprise over 150 mouse lines. Genotypic, phenotypic, and mRNA (mRNA) abundance data sets for these strains have been directly integrated into GeneNetwork's analytical platform, enabling open access to the data for the research community. To date, the database contains approximately 99 eye-related phenotypes, rendering it a well suited resource for ophthalmological research [11].

Using this platform, several novel molecular mechanisms underlying glaucoma, vascular retinopathies, and other ocular diseases have been identified [12-14]. Furthermore, the BXD panel has been extensively used to investigate the pathogenesis of complex metabolic disorders, including diabetes, obesity, and nonalcoholic fatty liver disease [15-17]. Thus, the BXD strain resource offers a unique platform for conducting TWAS studies to decipher the molecular mechanisms underlying DR.

In this study, we established a diabetic mouse model with impaired scotopic vision and performed label-free quantitative proteomic analysis on retinal tissues. Combined with TWAS analysis in BXD mouse strains, we identified retinal genes associated with blood glucose, which were enriched in the glutamate metabolism pathway. Furthermore, we investigated the glutamate receptor Grm6 at both the mRNA and protein levels. Finally, gene coexpression network analysis revealed the potential mechanisms by which glutamate accumulation induces scotopic vision impairment.

METHODS

Diabetic mouse model: Male C57BL/6J mice (6–8 weeks old) were housed in a specific pathogen–free (SPF) barrier system under controlled conditions: constant temperature (24 °C ± 1 °C), humidity (50% ± 10%), and a 12-h light–dark cycle. Mice had free access to standard chow diet (nutritional composition: crude protein ≥200 g/kg, crude fat ≥40 g/kg, crude fiber 50 g/kg, crude ash ≤80 g/kg, calcium 10–18 g/kg, total phosphorus 6–12 g/kg, lysine ≥13.2 g/kg, and methionine plus cystine ≥7.8 g/kg) and water. All experimental mice were healthy, with no ocular diseases. Animal experiments were approved by the animal research ethics committee at Binzhou Medical University (Approval No. 2021–200). The diabetic mouse model was induced by streptozotocin (STZ) administration [18]. STZ (S0130; Sigma, Shanghai, China) was dissolved in 0.1 mol/l sodium citrate buffer (pH 4.5) to a final concentration of 10 mg/ml. Mice received daily intraperitoneal injections of STZ (60 mg/kg) for 5 consecutive days, while control mice were injected with an equal volume of citrate buffer. Random blood glucose levels were measured using a glucometer with tail-vein blood samples. Diabetic mice were grouped and maintained for 1 month.

Electroretinograms: Mice were anesthetized via intraperitoneal injection of xylazine (14 mg/kg) and ketamine (60 mg/kg) and placed on a heating pad maintained at 37 °C. Prior to the experiment, pupils were dilated with 0.5% phenylephrine hydrochloride and 0.5% tropicamide eye drops, and the corneas were kept hydrated with 1% methylcellulose. ERG recordings were performed under standardized conditions. Following 24 h of dark adaptation, three mice per group were anesthetized under a deep-red LED light source with a peak wavelength of 660 nm in a dark room. ERG signals were recorded using a gold-plated wire ring electrode placed on the corneal surface, with stainless steel needle electrodes inserted subcutaneously near the eye (reference electrode) and in the tail (ground electrode), respectively. ERG data were acquired using a Reti-scan system (Roland Consult, Brandenburg an der Havel, Germany) with an amplifier, and parameters were set as follows: light intensity, 1.0 log cd·s/m2; sampling rate, 2 kHz.

Retinal proteome analysis: Seven pairs of mouse retinal tissues were subjected to label-free proteomic analysis as described in our previous studies [15,19]. Briefly, proteins were digested with trypsin (ADV5111; ThermoFisher Scientific, Waltham, MA) at a final concentration of 5% (w/w) overnight at 37 °C. The resulting peptides were analyzed by liquid chromatography/tandem mass spectrometry (Q Exactive Plus Orbitrap mass spectrometer, ThermoFisher Scientific). Proteomics raw data were processed by using

MaxQuant (version 1.5.0.1) against the UniProt *Mus musculus* database (release 2019–12). Differentially expressed proteins were visualized using volcano plots and heatmaps (Bioinformatics, Shanghai, China).

Quantitative reverse transcription polymerase chain reaction analyses: Mice were euthanized, and retinas were harvested to extract total RNA using a rapid RNA extraction kit (TR154–50; Tianmo Technology, Beijing, China). cDNA was synthesized using All-In-One 5× Master Mix (G592; ABM, Richmond, BC, Canada). Quantitative reverse transcription polymerase chain reaction was performed on a 7500 Real-Time PCR System (Thermo Fisher Scientific, Singapore) with the following cycling conditions: initial denaturation at 95 °C for 30 s, followed by 40 cycles of denaturation 95 °C for 10 s and annealing/extension at 60 °C for 30 s. Primers used were as follows: GAPDH-F: 5′-AAG AAG GTG GTG AAG CAA G-3′, GAPDH-R: 5′-GAA GGT GGA AGA GTG GGA GT-3′; GRM6-F: 5′-CGG ACC CTG CTG CAC TAC AT-3′, GRM6-R: 5′-CCC CAT TCT CAT TGA ACA TCA CT-3′.

Western blotting: Isolated retinal tissues were homogenized in lysis buffer (P0013B; Beyotime, Shanghai) containing a proteinase inhibitor. Total proteins were extracted by centrifugation at 16,114 × *g* for 15 min at 4 °C and quantified using the BCA method. For electrophoresis, 50 µg of protein per lane was loaded onto 7.5% sodium dodecyl sulfate–PAGE gels, followed by transfer to 0.2-µm polyvinylidene fluoride membranes. Membranes were blocked with 5% fat-free milk for 1 h at room temperature, then incubated overnight at 4 °C with the following primary antibodies: GRM6 (BF8980, 1:500; AFFINITY, Jiangsu, China), GAD1 (AF0163, 1:500; AFFINITY), and tubulin (AF7011, 1:1,000; AFFINITY). After three washes with TBST (0.1% Tween-20), membranes were incubated with the secondary antibody Goat Anti-Rabbit IgG-HRP (S001, 1:5,000; AFFINITY) for 1 h at room temperature. Following three additional TBST washes, signals were developed using an Affinity ECL kit (AFFINITY; KF8001, Jiangsu, China) and imaged with a chemiluminescence imager (ChemiScope 6200 Touch, Shanghai, China).

Glutamate level detection: Retinal glutamate levels were measured using a glutamate detection kit (BTK048; Bioswamp, Beijing, China). Fresh retinal tissues were homogenized in ice-cold normal saline (0.9% NaCl) of an appropriate volume using a tissue homogenizer. Homogenates were centrifuged at 12,000 × *g* for 15 min at 4 °C, and supernatants were collected. These supernatants were then filtered through a 10-kDa ultrafiltration tube by centrifugation. Filtrates were mixed with the working solution and incubated at 37 °C for 20 min. The optical density was measured at 470 nm, and glutamate levels in samples were calculated by comparing optical density values to a standard curve.

BXD retina transcriptomic data set: The BXD retinal transcriptome data set was retrieved from the GeneNetwork website (https://genenetwork.org/). The parameters were set as follows: Species, Mouse (mm10); Group, BXD Family; Type, Retina mRNA; Data Set, HEI Full Retina Illumina V6.2 (Apr 10) RankInv; and Get Any, Grm6. The transcriptome data set (ID: 3,162,125) was obtained. Data visualization was performed using GraphPad Prism 8.0 (GraphPad Software, La Jolla, CA) to display changes in Grm6 gene expression levels across BXD mice strains.

BXD mice blood glucose data set: Basal blood glucose phenotype data were retrieved from the GeneNetwork website. The parameters were set as follows: Species, Mouse (mm10); Group, BXD Family; Type, Phenotypes; Data Set, BXD Phenotypes; and Get Any, Basal glucose. The basal glucose data set (ID: BXD_17799) was obtained from 29-week-old BXD mice. These mice were maintained on a chow diet and fasted overnight, and basal blood glucose was measured from tail-vein blood samples using a glucometer. For each BXD strain, basal glucose values were averaged. The data set is accessible via GeneNetwork with record ID BXD_17799.

Analysis of the correlation between retinal genes and blood glucose: Pearson correlation coefficient analysis was performed to assess the correlation between retinal gene expression and basal blood glucose levels, with statistical significance defined as a $p<0.05$. Correlation calculations were conducted using GeneNetwork. The Pearson correlation coefficient (R) quantifies the strength and direction of the linear relationship between two variables, ranging from −1 to 1. Specifically, $R>0$ indicates a positive correlation, while $R<0$ indicates a negative correlation. Additionally, the closer the absolute value of R (|R|) is to 1, the stronger the linear correlation between the two variables.

Gene correlation analysis: The top 2,000 genes associated with Grm6 in the BXD mouse retina were retrieved from GeneNetwork using the BXD retinal transcriptome data set. Gene correlation analysis was then performed via the "Compute Correlation" function to confirm these associations.

Gene function enrichment analysis: Gene function enrichment analysis was performed using the WEB-based Gene SeT AnaLysis Toolkit (WebGestalt, Houston, TX). Basic parameters were set as follows: organism, "Mus musculus"; method, "ORA"; and Reference Set, "Genome protein-coding." Gene Ontology analysis covered the Biologic Process, Cellular Component, and Molecular Function. Kyoto Encyclopedia

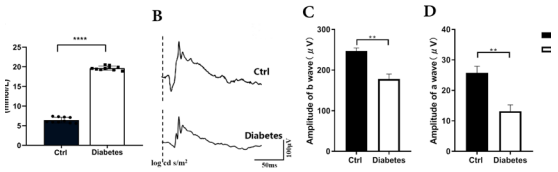

Figure 1. The diabetic mouse model shows impaired scotopic vision. **A**: The mice with diabetes for a month had higher random blood glucose levels than controls. n=10, ****p<0.0001. **B**–**D**: The representative electroretinographic statistical analysis in normal mice and diabetic mice shows that the amplitudes of the a- and b-waves in diabetic mice significantly decreased. n=6 eyes in each group. Data are shown as mean ± SD **p<0.01.

of Genes and Genomes (KEGG) pathway analysis was conducted to identify key pathways involved in scotopic vision impairment in diabetic mice [20].

Gene coexpression network analysis: A gene coexpression network was constructed as previously described [21,22]. Briefly, Pearson correlation coefficients for related genes were calculated based on the transcriptomic data set. Then, the network was built using the Pearson correlation coefficient matrix. In the network, each node represents a gene, and each edge denotes the correlation coefficient. A binomial correlation with an absolute value >0.25 (r >0.25 or r < −0.25) was defined as a connection.

Statistical analysis: A two-tailed Student *t* test was used to compare retinal protein expression levels between the diabetic and control groups to identify the significantly altered proteins (p<0.05). Correlation analysis was performed and visualized using GraphPad Prism software (8.0.1; GraphPad Software), with data sourced from the GeneNetwork database. A p value <0.05 was considered statistically significant.

RESULTS

Hyperglycemia induces scotopic vision impairment in mice: First, we established a diabetic mouse model through multiple administrations of low-dose STZ. Compared with control mice, diabetic mice displayed hyperglycemia, with random blood glucose levels exceeding 18.9 mM (Figure 1A). We then assessed retinal electrical activity using ERG. Recordings showed that b-wave amplitudes were significantly lower in diabetic mice than in controls (Figure 1B, C), indicating that scotopic vision was impaired in the diabetic retina. These results confirmed the successful establishment of a diabetic mouse model with impaired scotopic vision. Furthermore, analysis of ERG recordings revealed a significant reduction in a-wave amplitude in diabetic retinas (Figure 1D), suggesting impaired photoreceptor function.

Hyperglycemia alters retinal proteomic profiles: To investigate retinal protein expression patterns in diabetic mice, we performed label-free quantitative proteomic analysis on retinas from control and diabetic mice. A total of 1,770

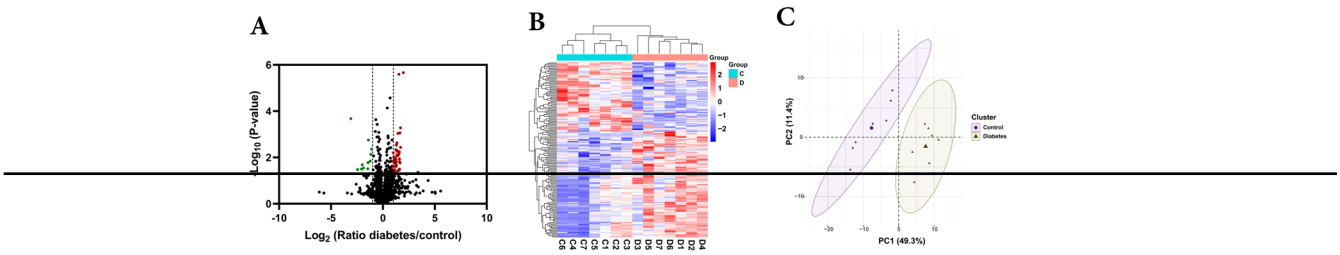

Figure 2. Hyperglycemia leads to changes in protein patterns in the retina. **A**: The differentially expressed proteins are shown by a volcano plot between the diabetic and control groups. The $-\log_{10}$ (p value) was plotted against the $\log_2$(ratio diabetes/control). The upregulated proteins (p<0.05) are labeled with red dots, and the downregulated proteins (p<0.05) are labeled with green dots. Proteins with no significant expression differences are marked in black. **B**: The 151 differentially expressed proteins (p<0.05) between the diabetic and control groups are shown by a heatmap. Red indicates the upregulated proteins, while blue represents the downregulated proteins. C, control group; D, diabetes group. **C**: Principal component (PC) analysis was performed based on the quantitative proteomics profiles of the retina. PC1 and PC2 were calculated and plotted. The clusters show the significant differences between diabetic and control mice.

proteins (from the UniProt database) were identified and quantified across all samples (Figure 2A, Appendix 1), among which 151 proteins were significantly differentially expressed ($p<0.05$): 92 were upregulated and 59 were downregulated in the retinas of diabetic mice (Figure 2B, Appendix 2). Principal component analysis revealed distinct separation of retinal proteomic profiles between diabetic and control mice (Figure 2C). Collectively, these proteomic results indicate that hyperglycemia alters retinal proteomic patterns and provide potential targets for exploring the molecular mechanisms by which hyperglycemia induces scotopic vision impairment.

Hyperglycemia induces aberrant glutamate metabolism and glutamate accumulation: During the initial phase of our study, proteomic analysis identified 151 differentially expressed proteins in the retina, and their corresponding coding genes were selected as candidate genes. To identify candidate genes associated with hyperglycemia, we performed a retinal TWAS between blood glucose and the transcripts of 151 differentially expressed proteins in BXD mouse strains using the GeneNetwork database. Among these candidates, 22 genes showed a significant correlation with blood glucose level ($p<0.05$; Figure 3A and Appendix 3). Furthermore, Gene Ontology term enrichment analysis of these 22 genes revealed enrichment in cellular components, including axons (Snap25, Gad1, Aldoc, Hspa8, Slc1a2, Amph, Cnga1), presynapses (Snap25, Gad1, Hspa8, Slc1a2, Amph, Cnga1), and the photoreceptor ribbon synapse cellular component (Hspa8, Amph; p=3.34E-06; Figure 3B). This suggests that the enriched genes (e.g., Snap25, Gad1, Hspa8, among others) play critical roles in maintaining the structural integrity of retinal axonal structures and regulating presynaptic transmission, which may mediate the initial stages of visual signal transduction from photoreceptors to bipolar cells. Additionally, KEGG pathway analysis identified the top three enriched pathways as necroptosis (Glud1, Slc25a4, Slc25a5; p=0.001), carbon metabolism (Aldoc, Glud1, Idh1; p=0.001), and alanine, aspartate, and glutamate metabolism (Slc1a2, Gad1, Glud1; p=0.003; Figure 3C). Hematoxylin and eosin staining revealed no obvious morphological abnormalities or signs of necroptosis in the retinal laminar structure (Appendix 4). Thus, we focused on the alanine, aspartate, and glutamate metabolism pathway, which was enriched with glutamate catabolism–related genes. Consistently, proteomics analysis showed that Slc1a2, Gad1, and Glud1 were downregulated in the diabetic retina (Figure 3D). Furthermore, at the transcript level, these three glutamate catabolism–related genes showed a significant negative correlation with blood glucose: Slc1a2 (R=–0.2925, p=0.0285), Gad1 (R=–0.3806, p=0.0059), and Glud1 (R=–0.2762, p=0.0466; Figure 3E–G). Western blot experiments confirmed the expression pattern of Gad1 protein, with results consistent with mass spectrometry analysis, showing decreased Gad1 protein expression in the retinas of diabetic mice (Figure 3H, I). Moreover, we measured retinal glutamate levels and found that glutamate accumulated in the retinas of diabetic mice (Figure 3J). These results demonstrated that hyperglycemia negatively regulates the expression of glutamate catabolism–related genes, leading to glutamate accumulation. Based on these findings, we subsequently investigated the glutamate metabolic pathway, which is closely associated with glutamate receptor–mediated signal transduction.

Glutamate accumulation induces downregulation of Grm6 expression in the retina of diabetic mice: To further explore the effects of glutamate accumulation on its receptors, we performed a correlation analysis between blood glucose and eight types of metabotropic glutamate receptors in the retinas of BXD mouse strains. Among these receptors, Grm6 showed the most significant correlation with blood glucose (R=–0.5291, p=0.0003; Figure 4A, B). In 43 BXD mouse strains, the average expression of Grm6 was 14.16±0.04 (log2 scale, mean ± standard error of the mean). The BXD67 strain exhibited the lowest expression (13.52±0.16), while the BXD24 strain showed the highest (15.84±0.14; Figure 4C). Among these strains, Grm6 expression varied significantly, with a fold change of 4.997 (Appendix 5). This indicates natural variation in Grm6 expression within the BXD genetic reference population, reflecting differences in expression levels shaped by genetic background and potential regulation by environmental factors. Furthermore, quantitative reverse transcription polymerase chain reaction and western blotting revealed decreased Grm6 mRNA and protein levels in the retinas of diabetic mice (Figure 4D–F). These findings suggest that Grm6, likely an environmentally sensitive gene, is downregulated in the diabetic mouse retina.

Grm6 is associated with glutamate accumulation–induced scotopic vision impairment via the phototransduction pathway: To explore the potential mechanism by which Grm6 contributes to glutamate accumulation–induced scotopic vision impairment, we screened the top 2,000 Grm6-coexpressed genes in the retina ($p<0.05$) for functional enrichment analysis. KEGG pathway enrichment results showed that the phototransduction pathway was the most significantly enriched (Figure 5A). To confirm the correlation between Grm6 and the phototransduction pathway, we calculated Pearson correlation coefficients between Grm6 and five phototransduction-related genes (Gnat1, Gucy2e, Cnga1, Grk1, Rgs9), all of which were also identified in our retinal proteome (Figure 5B). Correlation analysis revealed that Rgs9 had a significantly strong positive correlation with

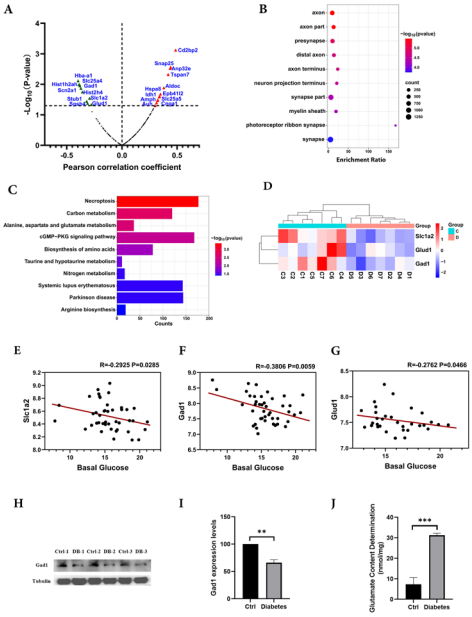

Figure 3. Hyperglycemia leads to aberrant glutamate metabolism. **A**: The correlations between retinal mRNA levels of differentially expressed proteins and the blood glucose level from BXD mice (Record ID17799) were evaluated, and 22 genes were significantly associated with the blood glucose level. The red triangles represent significant positive associations, the green triangles represent significant negative associations, and the dark plots represent no statistical significance. **B**: Gene Ontology analysis based on their Cellular Component (CC). The 22 genes were enriched in axon, axon part, and presynaptic. The size of the dots represents the number of genes, and the color indicates the p values. **C**: Kyoto Encyclopedia of Genes and Genomes pathway analysis shows that the top three enriched pathways included alanine, aspartate, and glutamate metabolism. The color represents the p values (WebGelstat). **D**: Three proteins (Slc1a2, Gad1 and Glud1) involved in glutamate metabolism, which were downregulated in the diabetic retina, are shown by a heatmap. The red indicates upregulated proteins, while blue represents downregulated proteins. C, control group; D, diabetes group. **E–G**: The scatterplots illustrate the correlations between blood glucose levels and the expression of three glutamate catabolism–related genes, including *slc1a2* (**E**), *gad1* (**F**), and *glud1* (**G**). The *R* and p values are shown in the figure. The gene expression data were $\log_2$-transformed in this analysis. **H–I**: western blot analysis shows that Gad1 protein expression was decreased in the diabetic mouse retina. **J**: The glutamate content in the mouse retina was measured using an enzyme-linked immunosorbent assay kit.

Grm6 (R=0.604, p=1.08E-9; Figure 5C). To illustrate the relationships among these factors, we constructed a correlation network including phototransduction-related genes (Gnat1, Gucy2e, Cnga1, Grk1, Rgs9), glutamate metabolism genes (Slc1a2, Gad1, Glud1), the glutamate receptor Grm6, and blood glucose levels (Figure 5D). Overall, the schematic diagram illustrates how Grm6 is involved in hyperglycemia-induced scotopic vision impairment (Figure 5E). Under hyperglycemic conditions, high glucose levels disrupt retinal glutamate metabolism by downregulating the expression of glutamate metabolic enzymes such as Gad1, leading to glutamate accumulation. This glutamate accumulation–induced toxicity downregulates Grm6 expression in rod bipolar cells. Network analysis identified a correlation between Grm6 and Rgs9, suggesting that hyperglycemia may impair scotopic vision via the phototransduction pathway. The combined disruption of these molecular networks and cellular pathways ultimately impairs scotopic vision.

DISCUSSION

It has been reported that scotopic vision loss is the first symptom of DR [23]. However, the molecular mechanisms underlying hyperglycemia-induced scotopic vision impairment remain unclear. To explore the potential links between hyperglycemia and scotopic vision impairment, we first performed label-free quantitative proteomic analysis on retinas from diabetic mice, identifying over 150 differentially expressed proteins. Verifying key proteins and pathways from hundreds of candidate proteins remains a challenge [24]. In this study, we integrated transcriptome-wide association analysis from over 150 BXD mouse strains with proteomic data, leading to the identification of a potentially dysregulated pathway: the alanine, aspartate, and glutamate

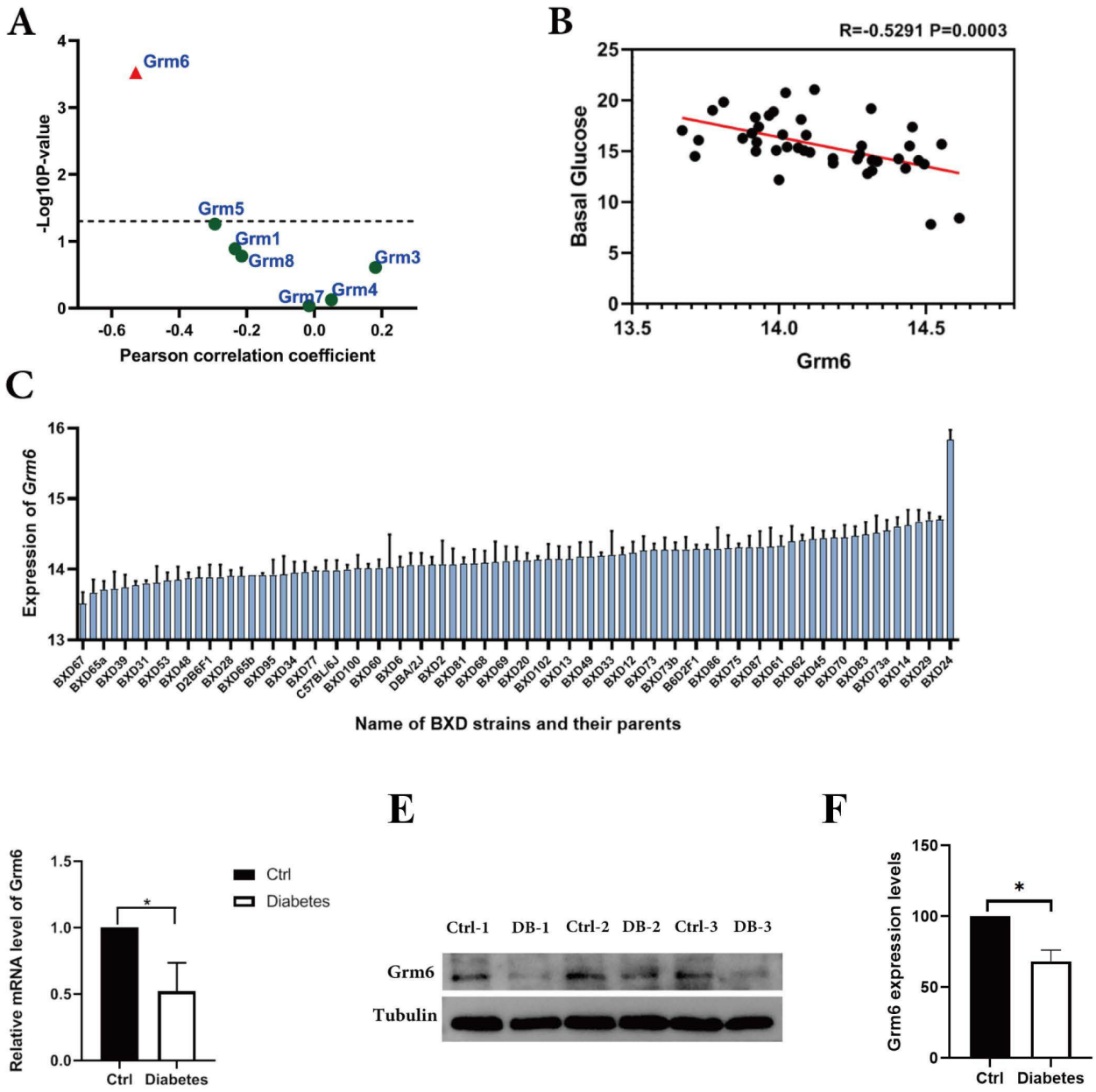

Figure 4. Grm6 expression is associated with the level of blood glucose. **A**: The volcano plot shows the correlations between blood glucose level and eight types of metabotropic glutamate receptors. The x-axis represents the Pearson correlation coefficient, and the y-axis represents the $-\log_{10}$ (p value). The receptor Grm6, marked with a red triangle, was most significantly correlated with blood glucose levels. **B**: The scatterplots show that the expression levels of Grm6 had a significantly negative correlation with the basal glucose level (R=–0.5291, p=0.0003). Each dark dot represents a mouse strain. **C**: The Grm6 expression varied in BXD strains and their parental strains (C57BL/6J and DBA/2J). The x-axis represents the name of BXD strains and their parents (C57BL/6J and DBA/2J), as well as two F1 strains (D2B6F1 and B6D2F1). The y-axis shows that the average expression level of Grm6 is 14.16±0.04 ($\log_2$ scale, mean ± standard error of the mean). Each bar is marked with a standard error of the mean. **D**: Quantitative reverse transcription polymerase chain reaction analysis shows that Grm6 expression was decreased significantly compared with the control group. **E**: western blot analysis shows that Grm6 expression was decreased in the protein level in diabetic mice retina. **F**: The quantitative analyses in E were performed by ImageJ 1.46 and GraphPad Prism 8. Data are shown as mean ± standard deviation. n=3. *p<0.05.

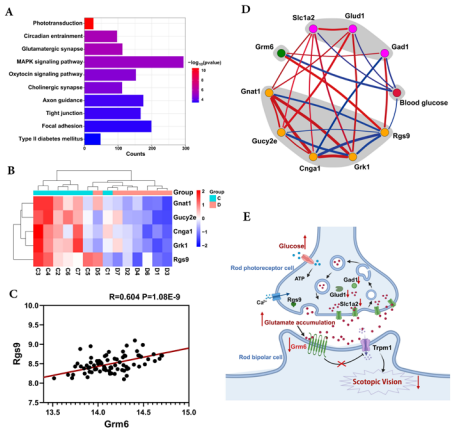

Figure 5. Grm6 is associated with hyperglycemia-induced scotopic vision impairment via the phototransduction pathway. **A**: The bar plots show the enriched Kyoto Encyclopedia of Genes and Genomes terms for the top 2,000 Grm6-associated genes in the BXD retinas. The x-axis indicates the number of genes, and the color represents the $-\log_{10}$ (p values). **B**: Five proteins (Gnat1, Gucy2e, Cnga1, Grk1, and Rgs9) involved in the phototransduction pathway, which were downregulated in the diabetic retina, are shown in a heatmap. Red indicates the upregulated proteins, while blue represents the downregulated proteins. C, control group; D, diabetes group. **C**. These scatterplots illustrate the correlations between *grm6* and *rgs9*. The *R* and p values are shown. The gene expression data were $\log_2$-transformed in this analysis. **D**: The network included the genes enriched in the phototransduction pathway (orange nodes), glutamate metabolism (purple nodes), glutamate receptor (green node), and blood glucose level (red node). The red and blue edges show significant positive and negative correlations, respectively ($p<0.05$). The thickness of the edges represents the Pearson correlation coefficient. **E**: Proposed model illustrates that Grm6 was involved in hyperglycemia-induced scotopic vision impairment. The hyperglycemia led to glutamate accumulation, which decreased *Grm6* expression. *Grm6* may affect the phototransduction pathway via *Rgs9*, leading to scotopic vision impairment.

metabolism pathway. Our study thus provides an efficient strategy for identifying critical proteins and pathways in retinal proteomics research.

Using this strategy, we found that the glutamate metabolism pathway is significantly dysregulated, with downregulation of the glutamate catabolism–related genes Slc1a2, Gad1, and Glud1 in the diabetic retina. Slc1a2 is the primary transporter responsible for clearing the excitatory neurotransmitter glutamate from the extracellular synaptic space [25]. Glutamate clearance is essential for normal synaptic activation and for preventing excitotoxicity, which triggers postsynaptic neuron death [25,26]. GLUD1 catalyzes the oxidative deamination of glutamate to α-ketoglutarate and ammonia, playing a key role in regulating glutamate metabolism [27]. GAD1 converts excitatory glutamate into the inhibitory neurotransmitter gamma-aminobutyric acid. Our previous study also demonstrated that exogenous GAD1 treatment enhances retinal ganglion cell survival in the optic nerve crush–injured retina [18]. In this study, we confirmed that hyperglycemia negatively regulates the expression of glutamate catabolism–related genes, leading to glutamate accumulation. These results are consistent with previous findings showing elevated retinal glutamate levels and increased toxicity to retinal neurons [28].

Glutamate accumulation exerts excitotoxic effects in the nervous system [29]. Neurodegeneration and neurologic dysfunction are early manifestations of diabetes, preceding primary retinal vasculopathy [30]. Hyperglycemia impairs retinal neuron function through multiple mechanisms, including abnormal Ca^{2+} homeostasis [31], metabolic disorder–induced changes in gene regulation in bipolar cells [32], and enhanced glutamate excitotoxicity [33]. Ca^{2+} plays a key role in neurotransmitter release. In diabetic amacrine cells, reduced calcium buffering decreases light-evoked inhibitory input from presynaptic GABAergic amacrine cells to rod bipolar cells [31]. Calcium is also critical for the function and survival of both rod and cone photoreceptors. For photoreceptors, rapid regulation of Ca^{2+} levels in their outer segments is essential for modulating phototransduction, which mediates the termination of flash responses and light adaptation in both rod and cone cells [34]. For example, Ca1.4 L-type calcium channels, predominantly expressed in photoreceptor terminals, are essential for synaptic transmission and vision. Their dysfunction is linked to congenital stationary night blindness (CSNB), a disease characterized by severe impairment of both scotopic and photopic vision [35]. Studies have also shown that intracellular Ca^{2+} levels are significantly elevated in rod cells from diabetic mice. This Ca^{2+} overload activates calpain 1, leading to oxidative stress, the expression of inflammatory proteins, and eventual photoreceptor

degeneration [36]. In diabetic retinal Müller cells, glutamate conversion to α-ketoglutarate via transamination is reduced by 90%, and glutamate accumulation triggers excitotoxicity [33]. Another study found that excessive free glutamate levels are associated with photoreceptor degeneration in a retinal degeneration mouse model [37].

Glutamate exerts its physiologic functions by binding to its receptors [29]. Among the eight known metabotropic glutamate receptors, our TWAS analysis identified a significant correlation between Grm6 and blood glucose levels. Studies have demonstrated that the Grm6 receptor, encoded by the Grm6 gene, is a key receptor specifically expressed on the surface of retinal ON bipolar cells, where it plays a central role in visual signal transmission [38,39]. It has been reported that loss of Grm6 leads to defects in signal transmission from photoreceptors to ON-bipolar cells, resulting in CSNB [40,41]. In this study, we also found decreased Grm6 expression in the diabetic retina. This further supports the association between Grm6 and glutamate accumulation–induced scotopic vision impairment in diabetic mice.

To further explore the potential mechanism of Grm6 signaling in the retina, we constructed a Grm6-centric gene coexpression network. Pathway analysis revealed that Grm6 is correlated with the phototransduction pathway via Rgs9. RGS9 is currently recognized to exist in two major isoforms: RGS9–1 and RGS9–2. RGS9–1, localized in photoreceptor cells, primarily regulates GTP hydrolysis on transducin in photoreceptor outer segments [42,43]. In contrast, RGS9–2 is predominantly expressed in axon terminals of the central nervous system, where it modulates μ-opioid receptor signaling in the periaqueductal gray by regulating G-protein activity, thereby influencing nociceptive behaviors and opioid responses [44]. Recent studies demonstrate that light-induced Gα translocation to rod synapses, mediated by Frmpd1, enhances synaptic transmission [45]. As a functional regulator coupled to Gα, RGS9 likely undergoes coordinated redistribution with Gα during phototransduction and light adaptation.

RGS9 acts as a calcium-dependent regulator of rhodopsin phosphorylation by GRK1 in response to light-dependent changes [42]. Additionally, studies have shown that RGS9 can also be phosphorylated by protein kinase A, and RGS9 phosphorylation requires free Ca^{2+} and is inhibited by light, suggesting that RGS9 phosphorylation may underlie the mechanism mediating a stronger photoresponse in dark-adapted cells [46]. Ca^{2+} influx through voltage-gated Ca^{2+} channels had been demonstrated to be both necessary and sufficient for triggering glutamate release [47,48]. Notably, metabotropic glutamate receptors play a key role in modulating intracellular calcium levels in neurons. Consistent with this, calcium imaging in isolated photoreceptors revealed that glutamate and class III metabotropic glutamate receptor agonists significantly reduce resting calcium levels [49]. Collectively, these findings suggest that Ca^{2+} may act as a dual regulator, coordinately modulating glutamate-mediated synaptic feedback and RGS9 function. This provides a rationale for further investigating RGS9 as a downstream effector in hyperglycemic retinopathy. Our study establishes the GRM6-glutamate axis as a key component of retinal signaling, with Rgs9 serving as a critical link between glutamate dysregulation and impaired phototransduction.

Phototransduction is the process by which absorbed light is converted into an electrical signal in photoreceptors. Photoreceptors are specialized neurons, including rods and cones, that transform light into neural signals and transmit them to the brain for image processing [50]. In the dark, rod cells are relatively depolarized, with light-sensitive channels activated, leading to continuous release of the neurotransmitter glutamate by photoreceptors [51,52]. Rods, acting as presynaptic elements, contact bipolar cells (postsynaptic elements) and transmit signals through glutamate receptors [26,53,54]. It has been reported that GRM6 plays a critical role in phototransduction within ON-bipolar (ON-BC) cells by mediating signal transmission from photoreceptors [55]. In the ON pathway, GRM6 forms a complex with downstream effectors (e.g., TRPM1) to transduce glutamate signals from photoreceptors into depolarizing responses [56]. GRM6 interacts with GPR179 and LRIT3 to ensure proper synaptic connectivity between photoreceptors and ON-BCs, and its dysfunction disrupts this cascade, impairing scotopic vision [50,57]. Additionally, GRM6 variants (p.Arg621Ter, p.Gly51Val, and p.Gly464Arg) cause autosomal recessive CSNB via pseudodominant inheritance, highlighting its essential role in phototransduction [58]. Mutations in Grm6 lead to CSNB, characterized by loss of the b-wave in ERGs and mislocalization of key proteins such as GPR179, TRPM1, and regulatory proteins (RGS7, RGS11) at ON-BC dendritic tips [55,59]. Based on the functional homology between RGS7/RGS11 and RGS9, combined with our findings demonstrating a strong correlation between Grm6 and RGS9, we hypothesize that the significant positive correlation between Grm6 and Rgs9, both involved in phototransduction, contributes to the pathogenesis of DR. However, the complexity of DR pathophysiology likely involves multiple pathways and genes contributing to scotopic vision impairment. Advanced multiomics approaches and well characterized animal models could help dissect these mechanisms, potentially paving the way for targeted therapies for diabetic retinal dysfunction.

Due to the limitations of mass spectrometry sequencing depth, Grm6 expression was not detected in the proteomic analysis. Therefore, future in-depth proteomics studies will provide more detailed insights to elucidate the mechanisms underlying diabetic scotopic vision impairment.

Conclusions: In summary, our study indicates that Grm6 is associated with scotopic vision impairment induced by glutamate accumulation. We propose that hyperglycemia-induced glutamate accumulation downregulates Grm6 expression, and Grm6 is correlated with Rgs9 in the phototransduction pathway, collectively contributing to scotopic vision impairment. Furthermore, our integrated strategy combining proteomics and TWAS analysis provides an efficient approach for identifying critical biomarkers and pathways in diabetic retinopathy research.

APPENDIX 1. SUPPLEMENTARY TABLE 1.

To access the data, click or select the words "Appendix 1." The total expressed proteins identified in Diabetic and Control retinal tissues.

APPENDIX 2. SUPPLEMENTARY TABLE 2.

To access the data, click or select the words "Appendix 2." Differentially expressed proteins identified in diabetic and control retinal tissues.

APPENDIX 3. SUPPLEMENTARY TABLE 3.

To access the data, click or select the words "Appendix 3." The correlation analysis between blood glucose level and the transcripts of 151 candidate proteins.

APPENDIX 4. SUPPLEMENTARY FIGURE 1.

To access the data, click or select the words "Appendix 4." H&E staining of retinal tissues in control and diabetic mice. (A) Retina of a control mouse. (B) Retina of a diabetic mouse.

APPENDIX 5. SUPPLEMENTARY FIGURE 2.

To access the data, click or select the words "Appendix 5." Basic statistical information of the transcription levels of Grm6 under various strains.

ACKNOWLEDGMENTS

Financial support: This work was supported by grants from Key R&D Program of Shandong Province, China (No. 2023CXPT012), Major Basic Research Project of Shandong Provincial Natural Science Foundation (No. ZR2019ZD27), Shandong Province Higher Educational Youth Innovation Science and Technology Program (No.2019KJE013, 2021KJ052). Dr. Yanping Zhu (yanpingzhu1983@163.com) and Dr. Geng Tian (tiangeng@live.se) are co-corresponding authors for this study.

REFERENCES

1. Ghamdi AHA. Clinical Predictors of Diabetic Retinopathy Progression; A Systematic Review. Curr Diabetes Rev 2020; 16:242-7. [PMID: 30767747].
2. Lin KY, Hsih WH, Lin YB, Wen CY, Chang TJ. Update in the epidemiology, risk factors, screening, and treatment of diabetic retinopathy. J Diabetes Investig 2021; 12:1322-5. [PMID: 33316144].
3. Yau JW, Rogers SL, Kawasaki R, Lamoureux EL, Kowalski JW, Bek T, Chen SJ, Dekker JM, Fletcher A, Grauslund J, Haffner S, Hamman RF, Ikram MK, Kayama T, Klein BE, Klein R, Krishnaiah S, Mayurasakorn K, O'Hare JP, Orchard TJ, Porta M, Rema M, Roy MS, Sharma T, Shaw J, Taylor H, Tielsch JM, Varma R, Wang JJ, Wang N, West S, Xu L, Yasuda M, Zhang X, Mitchell P, Wong TY. Meta-Analysis for Eye Disease (META-EYE) Study Group. Global prevalence and major risk factors of diabetic retinopathy. Diabetes Care 2012; 35:556-64. [PMID: 22301125].
4. Ting DS, Cheung GC, Wong TY. Diabetic retinopathy: global prevalence, major risk factors, screening practices and public health challenges: a review. Clin Exp Ophthalmol 2016; 44:260-77. [PMID: 26716602].
5. Fan Y, Lai J, Yuan Y, Wang L, Wang Q, Yuan F. Taurine Protects Retinal Cells and Improves Synaptic Connections in Early Diabetic Rats. Curr Eye Res 2020; 45:52-63. [PMID: 31404506].
6. Bandello F, Cicinelli MV. 19th EURETINA Congress Keynote Lecture: Diabetic Retinopathy Today. Ophthalmologica 2020; 243:163-71. [PMID: 32015239].
7. de Moraes G, Layton CJ. Therapeutic targeting of diabetic retinal neuropathy as a strategy in preventing diabetic retinopathy. Clin Exp Ophthalmol 2016; 44:838-52. [PMID: 27334889].
8. McAnany JJ, Park JC. Rod photoreceptor activation and deactivation in early-stage diabetic eye disease. Doc Ophthalmol 2023; 146:229-39. [PMID: 36763216].
9. Pandiyan VP, Nguyen PT, Pugh EN Jr, Sabesan R. Human cone elongation responses can be explained by photoactivated cone opsin and membrane swelling and osmotic response to phosphate produced by RGS9-catalyzed GTPase. Proc Natl Acad Sci U S A 2022; 119:e2202485119[PMID: 36122241].
10. Gao J, Collyer J, Wang M, Sun F, Xu F. Genetic Dissection of Hypertrophic Cardiomyopathy with Myocardial RNA-Seq. Int J Mol Sci 2020; 21:3040-[PMID: 32344918].
11. Druka A, Druka I, Centeno AG, Li H, Sun Z, Thomas WT, Bonar N, Steffenson BJ, Ullrich SE, Kleinhofs A, Wise RP, Close TJ, Potokina E, Luo Z, Wagner C, Schweizer GF, Marshall DF, Kearsey MJ, Williams RW, Waugh R. Towards

systems genetic analyses in barley: Integration of phenotypic, expression and genotype data into GeneNetwork. BMC Genet 2008; 9:73-[PMID: 19017390].

12. Li S, Xu F, Liu L, Ju R, Bergquist J, Zheng QY, Mi J, Lu L, Li X, Tian G. A systems genetics approach to revealing the *Pdgfb* molecular network of the retina. Mol Vis 2020; 26:459-71. [PMID: 32587457].

13. Stiemke AB, Sah E, Simpson RN, Lu L, Williams RW, Jablonski MM. Systems Genetics of Optic Nerve Axon Necrosis During Glaucoma. Front Genet 2020; 11:31-[PMID: 32174956].

14. Chaum E, Winborn CS, Bhattacharya S. Genomic regulation of senescence and innate immunity signaling in the retinal pigment epithelium. Mamm Genome 2015; 26:210-21. [PMID: 25963977].

15. Zhu Y, Zhang C, Xu F, Zhao M, Bergquist J, Yang C, Liu X, Tan Y, Wang X, Li S, Jiang W, Ong Q, Lu L, Mi J, Tian G. System biology analysis reveals the role of voltage-dependent anion channel in mitochondrial dysfunction during non-alcoholic fatty liver disease progression into hepatocellular carcinoma. Cancer Sci 2020; 111:4288-302. [PMID: 32945042].

16. Williams EG, Wu Y, Jha P, Dubuis S, Blattmann P, Argmann CA, Houten SM, Amariuta T, Wolski W, Zamboni N, Aebersold R, Auwerx J. Systems proteomics of liver mitochondria function. Science 2016; 352:aad0189[PMID: 27284200].

17. Wang X, Pandey AK, Mulligan MK, Williams EG, Mozhui K, Li Z, Jovaisaite V, Quarles LD, Xiao Z, Huang J, Capra JA, Chen Z, Taylor WL, Bastarache L, Niu X, Pollard KS, Ciobanu DC, Reznik AO, Tishkov AV, Zhulin IB, Peng J, Nelson SF, Denny JC, Auwerx J, Lu L, Williams RW. Joint mouse-human phenome-wide association to test gene function and disease risk. Nat Commun 2016; 7:10464-[PMID: 26833085].

18. Furman BL. Streptozotocin-Induced Diabetic Models in Mice and Rats. Curr Protoc 2021; 1:e78[PMID: 33905609].

19. Zhu Y, Zhang Y, Qi X, Lian Y, Che H, Jia J, Yang C, Xu Y, Chi X, Jiang W, Li Y, Mi J, Yang Y, Li X, Tian G. GAD1 alleviates injury-induced optic neurodegeneration by inhibiting retinal ganglion cell apoptosis. Exp Eye Res 2022; 223:109201[PMID: 35940240].

20. Bu D, Luo H, Huo P, Wang Z, Zhang S, He Z, Wu Y, Zhao L, Liu J, Guo J, Fang S, Cao W, Yi L, Zhao Y, Kong L. KOBAS-i: intelligent prioritization and exploratory visualization of biological functions for gene enrichment analysis. Nucleic Acids Res 2021; 49:W1W317-25. [PMID: 34086934].

21. Zhou Y, Li H, Liu X, Chi X, Gu Z, Cui B, Bergquist J, Wang B, Tian G, Yang C, Xu F, Mi J. The Combination of Quantitative Proteomics and Systems Genetics Analysis Reveals that PTN Is Associated with Sleep-Loss-Induced Cognitive Impairment. J Proteome Res 2023; 22:2936-49. [PMID: 37611228].

22. Deng T, Li J, Liu J, Xu F, Liu X, Mi J, Bergquist J, Wang H, Yang C, Lu L, Song X, Yao C, Tian G, Zheng QY. Hippocampal Transcriptome-Wide Association Study Reveals Correlations Between Impaired Glutamatergic Synapse Pathway and Age-Related Hearing Loss in BXD-Recombinant Inbred Mice. Front Neurosci 2021; 15:745668[PMID: 34867157].

23. Eggers ED, Carreon TA. The effects of early diabetes on inner retinal neurons. Vis Neurosci 2020; 37:E006[PMID: 32933604].

24. Legati A, Giacopuzzi E, Spinazzi M, Lek M. Editorial: Application of Omics Approaches to the Diagnosis of Genetic Neurological Disorders. Front Neurol 2021; 12:712010[PMID: 34305806].

25. Green JL, Dos Santos WF, Fontana ACK. Role of glutamate excitotoxicity and glutamate transporter EAAT2 in epilepsy: Opportunities for novel therapeutics development. Biochem Pharmacol 2021; 193:114786[PMID: 34571003].

26. Klotz-Weigand L, Enz R. Metabotropic Glutamate Receptors at Ribbon Synapses in the Retina and Cochlea. Cells 2022; 11:1097-[PMID: 35406660].

27. Hohnholt MC, Andersen VH, Andersen JV, Christensen SK, Karaca M, Maechler P, Waagepetersen HS. Glutamate dehydrogenase is essential to sustain neuronal oxidative energy metabolism during stimulation. J Cereb Blood Flow Metab 2018; 38:1754-68. [PMID: 28621566].

28. Kowluru RA, Engerman RL, Case GL, Kern TS. Retinal glutamate in diabetes and effect of antioxidants. Neurochem Int 2001; 38:385-90. [PMID: 11222918].

29. Wang J, Wang F, Mai D, Qu S. Molecular Mechanisms of Glutamate Toxicity in Parkinson's Disease. Front Neurosci 2020; 14:585584[PMID: 33324150].

30. Flood MD, Wellington AJ, Cruz LA, Eggers ED. Early diabetes impairs ON sustained ganglion cell light responses and adaptation without cell death or dopamine insensitivity. Exp Eye Res 2020; 200:108223[PMID: 32910942].

31. Moore-Dotson JM, Eggers ED. Reductions in Calcium Signaling Limit Inhibition to Diabetic Retinal Rod Bipolar Cells. Invest Ophthalmol Vis Sci 2019; 60:4063-73. PMID: 31560762[PMID: 31560762].

32. Van Hove I, De Groef L, Boeckx B, Modave E, Hu TT, Beets K, Etienne I, Van Bergen T, Lambrechts D, Moons L, Feyen JHM, Porcu M. Single-cell transcriptome analysis of the Akimba mouse retina reveals cell-type-specific insights into the pathobiology of diabetic retinopathy. Diabetologia 2020; 63:2235-48. [PMID: 32734440].

33. Gowda K, Zinnanti WJ, LaNoue KF. The influence of diabetes on glutamate metabolism in retinas. J Neurochem 2011; 117:309-20. [PMID: 21288239].

34. Vinberg F, Chen J, Kefalov VJ. Regulation of calcium homeostasis in the outer segments of rod and cone photoreceptors. Prog Retin Eye Res 2018; 67:87-101. [PMID: 29883715].

35. Zanetti L, Kilicarslan I, Netzer M, Babai N, Seitter H, Koschak A. Function of cone and cone-related pathways in $Ca_V1.4$ IT mice. Sci Rep 2021; 11:2732-[PMID: 33526839].

36. Saadane A, Du Y, Thoreson WB, Miyagi M, Lessieur EM, Kiser J, Wen X, Berkowitz BA, Kern TS. Photoreceptor Cell Calcium Dysregulation and Calpain Activation Promote

Pathogenic Photoreceptor Oxidative Stress and Inflammation in Prodromal Diabetic Retinopathy. Am J Pathol 2021; 191:1805-21. [PMID: 34214506].

37. Delyfer MN, Forster V, Neveux N, Picaud S, Léveillard T, Sahel JA. Evidence for glutamate-mediated excitotoxic mechanisms during photoreceptor degeneration in the rd1 mouse retina. Mol Vis 2005; 11:688-96. [PMID: 16163266].

38. Masu M, Iwakabe H, Tagawa Y, Miyoshi T, Yamashita M, Fukuda Y, Sasaki H, Hiroi K, Nakamura Y, Shigemoto R. Specific deficit of the ON response in visual transmission by targeted disruption of the mGluR6 gene. Cell 1995; 80:757-65. [PMID: 7889569].

39. Dryja TP, McGee TL, Berson EL, Fishman GA, Sandberg MA, Alexander KR, Derlacki DJ, Rajagopalan AS. Night blindness and abnormal cone electroretinogram ON responses in patients with mutations in the GRM6 gene encoding mGluR6. Proc Natl Acad Sci U S A 2005; 102:4884-9. [PMID: 15781871].

40. Zeitz C, van Genderen M, Neidhardt J, Luhmann UF, Hoeben F, Forster U, Wycisk K, Mátyás G, Hoyng CB, Riemslag F, Meire F, Cremers FP, Berger W. Mutations in GRM6 cause autosomal recessive congenital stationary night blindness with a distinctive scotopic 15-Hz flicker electroretinogram. Invest Ophthalmol Vis Sci 2005; 46:4328-35. [PMID: 16249515].

41. Naeem MA, Gottsch AD, Ullah I, Khan SN, Husnain T, Butt NH, Qazi ZA, Akram J, Riazuddin S, Ayyagari R, Hejtmancik JF, Riazuddin SA. Mutations in GRM6 identified in consanguineous Pakistani families with congenital stationary night blindness. Mol Vis 2015; 21:1261-71. [PMID: 26628857].

42. Hu G, Jang GF, Cowan CW, Wensel TG, Palczewski K. Phosphorylation of RGS9–1 by an endogenous protein kinase in rod outer segments. J Biol Chem 2001; 276:22287-95. [PMID: 11292825].

43. Bernier SC, Millette MA, Roy S, Cantin L, Coutinho A, Salesse C. Structural information and membrane binding of truncated RGS9–1 Anchor Protein and its C-terminal hydrophobic segment. Biochim Biophys Acta Biomembr 2021; 1863:183566[PMID: 33453187].

44. Fullerton EF, Karom MC, Streicher JM, Young LJ, Murphy AZ. Age-Induced Changes in μ-Opioid Receptor Signaling in the Midbrain Periaqueductal Gray of Male and Female Rats. J Neurosci 2022; 42:6232-42. [PMID: 35790399].

45. Campla CK, Bocchero U, Strickland R, Nellissery J, Advani J, Ignatova I, Srivastava D, Aponte AM, Wang Y, Gumerson J, Martemyanov K, Artemyev NO, Pahlberg J, Swaroop A. Frmpd1 Facilitates Trafficking of G-Protein Transducin and Modulates Synaptic Function in Rod Photoreceptors of Mammalian Retina. eNeuro 2022; 9:ENEURO.0348–22[PMID: 36180221].

46. Balasubramanian N, Levay K, Keren-Raifman T, Faurobert E, Slepak VZ. Phosphorylation of the regulator of G protein signaling RGS9–1 by protein kinase A is a potential mechanism of light- and Ca^{2+}-mediated regulation of G protein function in photoreceptors. Biochemistry 2001; 40:12619-27. [PMID: 11601986].

47. Zhang M, Hu H, Zhang X, Lu W, Lim J, Eysteinsson T, Jacobson KA, Laties AM, Mitchell CH. The A3 adenosine receptor attenuates the calcium rise triggered by NMDA receptors in retinal ganglion cells. Neurochem Int 2010; 56:35-41. [PMID: 19723551].

48. Copenhagen DR, Jahr CE. Release of endogenous excitatory amino acids from turtle photoreceptors. Nature 1989; 341:536-9. [PMID: 2477707].

49. Krizaj D, Copenhagen DR. Calcium regulation in photoreceptors. Front Biosci 2002; 7:d2023-44. [PMID: 12161344].

50. Furukawa T, Ueno A, Omori Y. Molecular mechanisms underlying selective synapse formation of vertebrate retinal photoreceptor cells. Cell Mol Life Sci 2020; 77:1251-66. [PMID: 31586239].

51. Hack I, Peichl L, Brandstätter JH. An alternative pathway for rod signals in the rodent retina: rod photoreceptors, cone bipolar cells, and the localization of glutamate receptors. Proc Natl Acad Sci U S A 1999; 96:14130-5. [PMID: 10570210].

52. Schneider FM, Mohr F, Behrendt M, Oberwinkler J. Properties and functions of TRPM1 channels in the dendritic tips of retinal ON-bipolar cells. Eur J Cell Biol 2015; 94:420-7. [PMID: 26111660].

53. Nomura A, Shigemoto R, Nakamura Y, Okamoto N, Mizuno N, Nakanishi S. Developmentally regulated postsynaptic localization of a metabotropic glutamate receptor in rat rod bipolar cells. Cell 1994; 77:361-9. [PMID: 8181056].

54. Armata IA, Giompres P, Smith A, Stasi K, Kouvelas ED, Mitsacos A. Genetically induced retinal degeneration leads to changes in metabotropic glutamate receptor expression. Neurosci Lett 2006; 393:12-7. [PMID: 16213654].

55. Varin J, Bouzidi N, Dias MMS, Pugliese T, Michiels C, Robert C, Desrosiers M, Sahel JA, Audo I, Dalkara D, Zeitz C. Restoration of mGluR6 Localization Following AAV-Mediated Delivery in a Mouse Model of Congenital Stationary Night Blindness. Invest Ophthalmol Vis Sci 2021; 62:24-[PMID: 33729473].

56. Dhingra A, Sulaiman P, Xu Y, Fina ME, Veh RW, Vardi N. Probing neurochemical structure and function of retinal ON bipolar cells with a transgenic mouse. J Comp Neurol 2008; 510:484-96. [PMID: 18671302].

57. Delle Fave M, Cordonnier M, Vallee L, Condroyer C, Zeitz C, Balikova I. Congenital stationary night blindness in a patient with mild learning disability due to a compound heterozygous microdeletion of 15q13 and a missense mutation in *TRPM1*. Ophthalmic Genet 2021; 42:296-9. [PMID: 33691579].

58. Liu HY, Huang J, Xiao H, Zhang MJ, Shi FF, Jiang YH, Du H, He Q, Wang ZY. Pseudodominant inheritance of autosomal recessive congenital stationary night blindness in one family with three co-segregating deleterious GRM6

variants identified by next-generation sequencing. Mol Genet Genomic Med 2019; 7:e952[PMID: 31677249].

59. Orhan E, Neuillé M, de Sousa Dias M, Pugliese T, Michiels C, Condroyer C, Antonio A, Sahel JA, Audo I, Zeitz C. A New Mouse Model for Complete Congenital Stationary Night Blindness Due to *Gpr179* Deficiency. Int J Mol Sci 2021; 22:22-[PMID: 33922602].

Articles are provided courtesy of Emory University and The Abraham J. & Phyllis Katz Foundation. The print version of this article was created on 10 November 2025. This reflects all typographical corrections and errata to the article through that date. Details of any changes may be found in the online version of the article.